Accepted Manuscript

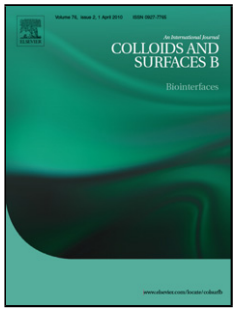

Title: Linoleic and linolenic acid hydroperoxides interact differentially with biomimetic plant membranes in a lipid specific manner

Authors: Magali Deleu, Estelle Deboever, Mehmet Nail Nasir, Jean-Marc Crowet, Manuel Dauchez, Marc Ongena, Haïssam Jijakli, Marie-Laure Fauconnier, Laurence Lins

PII: S0927-7765(18)30893-2
DOI: https://doi.org/10.1016/j.colsurfb.2018.12.014
Reference: COLSUB 9868

To appear in: *Colloids and Surfaces B: Biointerfaces*

Received date: 6 September 2018
Revised date: 29 November 2018
Accepted date: 6 December 2018

Please cite this article as: Deleu M, Deboever E, Nasir MN, Crowet J-Marc, Dauchez M, Ongena M, Jijakli H, Fauconnier M-Laure, Lins L, Linoleic and linolenic acid hydroperoxides interact differentially with biomimetic plant membranes in a lipid specific manner, *Colloids and Surfaces B: Biointerfaces* (2018), https://doi.org/10.1016/j.colsurfb.2018.12.014

Linoleic and linolenic acid hydroperoxides interact differentially with biomimetic plant membranes in a lipid specific manner

Magali Deleu[1*#], Estelle Deboever[1,2*], Mehmet Nail Nasir[1,2*], Jean-Marc Crowet[1,4], Manuel Dauchez[4], Marc Ongena[3], Haïssam Jijakli[5], Marie-Laure Fauconnier[2§] and Laurence Lins[1§]

[1]Laboratory of Molecular Biophysics at Interfaces, Gembloux Agro-Bio Tech, University of Liege, 2, Passage des Déportés, B-5030 Gembloux, Belgium

[2] Laboratoire de Chimie Générale et Organique, Gembloux Agro-Bio Tech, University of Liege, 2, Passage des Déportés, B-5030 Gembloux, Belgium

[3]Microbial Processes and Interactions Laboratory (MiPI), Gembloux Agro-Bio Tech, University of Liege, 2, Passage des Déportés, B-5030 Gembloux, Belgium

[4]Université de Reims Champagne-Ardenne, UMR CNRS 7369, "Matrice Extracellulaire et Dynamique Cellulaire", « Chaire MAgICS », UFR Sciences Exactes et Naturelles, Chemin des Rouliers, 51100 Reims, France.

[5]Laboratoire de Phytopathologie Intégrée et Urbaine, Gembloux Agro-Bio Tech, University of Liege, 2, Passage des Déportés, B-5030 Gembloux, Belgium

* : These authors have equally contributed to this work and must be considered as co-first authors.

§ : These authors have equally contributed to this work and must be considered as co-last authors.

[#] Corresponding author : magali.deleu@uliege.ac.be

Graphical abstract

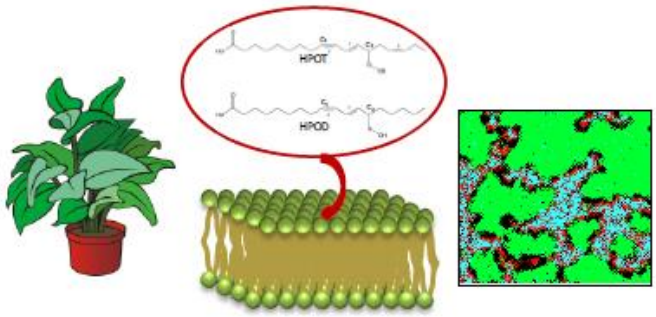

Highlights:

- Key intermediate oxylipins interact with plant plasma membrane models
- The interaction modifies the membrane lateral domains
- Hydrophobic effect and polar interactions are involved in the binding
- Chemical structure of hydroperoxides influences their affinity for plant membranes

Abstract

Linoleic and linolenic acid hydroperoxides (HPOs) constitute key intermediate oxylipins playing an important role as signaling molecules during plant defense processes in response to biotic or abiotic stress. They have also been demonstrated *in vitro* as antimicrobial agents against plant fungi and bacteria. To reach the phytopathogens *in vivo*, the HPOs biosynthesized in the plant cells must cross the plant plasma membrane (PPM) where they can also interact with plasma membrane lipids and have an effect on their organization.

In the present study, we have investigated the interaction properties of HPOs with PPM at a molecular level using biophysical tools combining *in vitro* and *in silico* approaches and using plant biomimetic lipid systems.

Our results have shown that HPOs are able to interact with PPM lipids and perturb their lateral organization. Glucosylceramide (GluCer) is a privileged partner, sitosterol lessens their binding and the presence of both GluCer and sitosterol further reduces their interaction. Hydrophobic effect and polar interactions are involved in the binding.

The chemical structure of HPOs influences their affinity for PPM lipids. The presence of three double bonds in the HPO molecule gives rise to a higher affinity comparatively to two double bonds, which can be explained by their differential interaction with the lipid polar headgroups.

Keywords: Oxylipins; plant membrane; molecular interactions; lipid specificity.

1. Introduction

Plants oxylipins are a group of molecules coming from the oxidative catabolism of poly unsaturated fatty acids (PUFAs) such as linoleic and α-linolenic acids [1–3] and known to play a role as signaling molecules during plant defense processes in response to biotic or abiotic stress [4–6]. The lipoxygenase (LOX), an enzyme frequently localized in the cytoplasm and catalyzing the first step of oxylipin pathway, converts polyunsaturated fatty acids (PUFAs) with 1-4 pentadiene structure to fatty-acid hydroperoxides (HPOs), such as 9 or 13-hydroperoxy-9,11,15-octadecatrienoic acid (HPOT) from α-linolenic and 9 or 13-hydroperoxy- 9,11-octadecadienoic acid (HPOD) from linoleic acid [7–10] (Figure 1). Following the reaction of LOX, these HPOs can be converted by at least seven diverging enzymatic pathways into various biologically active compounds differing in their chemical structures [2,5]. Among them, the pathway of 13-HPOs generates oxylipins very well characterized in the literature such as jasmonic acid, cis-12-oxo-phytodienoic acid (OPDA), cis-dinor-12-oxo-phytodienoic acid (*dn*-OPDA) or traumatic acid, indicating that 13-HPOs constitute key intermediate oxylipins [4]. Even though HPOs are principally converted into other oxylipins, free HPOs are also detected in plants [11].

In addition to their precursor role in the oxylipin pathways, HPOs have been demonstrated *in vitro* as antimicrobial agents against plant fungi and bacteria [12,13]. In terms of mechanism of action, Prost *et al.* have proposed that fatty acid derivatives like HPOs could exert their antimicrobial activity through interactions with pathogen biological membranes [12]. In this context, the antimicrobial effects of 13-HPOD have been analyzed on yeast and found to be linked to a strong interaction of this compound with the cell membrane lipids [14]. 13-HPOD can fluidize yeast plasma membranes inducing a biocide effect [14]. It has hence been suggested that HPOs exert their biological activity against different microbes by interacting with their membrane lipids [12].

To reach the phytopathogens, the HPOs biosynthesized in the plant cells must cross the plant plasma membrane (PPM). At that location, they may also interact with plant membrane lipids and could have an effect on their organization. To our best knowledge, the interactions of HPOs with plant lipids have not yet been analyzed at the molecular level, nor in the light of their conformation and/or lipid specificity.

The aim of the present paper is to answer to three main questions:

i) Is there any interaction between PPM lipids and HPOs?

ii) Is there any lipid specificity in these potential interactions?

iii) Do 13-HPOT and 13-HPOD similarly behave with PPM lipids?

The investigation was conducted using biophysical tools combining *in vitro* and *in silico* approaches and using plant biomimetic lipid systems.

2. Materials & Methods

2.1. Materials

Palmitoyl-2-linoleoyl-sn-glycero-3-phosphocholine (PLPC), sitosterol and D-glucosyl-ß-1,1'-N-palmitoyl-D-erythro-sphingosine (d18:1/16:0) (Glucosylceramide or GluCer) were purchased from Avanti Polar Lipids and used without further purification. Deuterium oxide (D_2O) at 99.9% isotopic purity, dimethylsulfoxide (DMSO) and Tris(hydroxymethyl)aminomethane (Tris) were provided from Sigma Chemical Co. The ultrapure water was produced by a Millipore system available in our laboratory, the resistivity was 18.2 Ω cm. Chloroform and methanol were both purchased from Scharlau Lab Co. The lipoxidase from *Glycine max* (soybean) type I-B (LOX-1), the α-linolenic and linoleic acids were purchased from Sigma- Aldrich.

2.2. Synthesis of HPOs

13-*S*-HPOT and 13-*S*-HPOD were obtained by the enzymatic reaction of soybean LOX-1 on linolenic and linoleic acid, respectively as described previously [15]. The HPLC-DAD purity of the molecules was superior to 95% and their structure was checked by NMR.

2.3. Experiments using Langmuir technology

For the adsorption experiments at constant surface area, the balance built by KSV (Helsinki, Finland) placed on a vibration-isolated table was equipped with a Wilhelmy plate. Adsorption experiments were performed in a KSV Minitrough (190 cm^3) in the absence or in the presence of lipids at the interface as described previously [16]. The subphase was 10mM Tris buffer at pH 7.4 prepared with ultrapure water with a constant temperature at 25°C. The subphase was continuously stirred with a magnetic stirrer. Lipid molecules in chloroform/methanol (2/1, v/v) mixture were spread at the air-water interface in order to reach desired initial surface pressure. After 30 minutes-waiting for solvent evaporation and film

stabilization, HPOs dissolved in DMSO were injected underneath the pre-formed lipid monolayer to final concentration of 12.7 µM in the subphase, i.e. at a concentration below the critical micellar concentration of HPO which is 25.4 ± 1.9 µM and 24.0 ± 1.3 µM for HPOT and HPOD respectively (see Figure S1) in order to have HPOs in a monomer form. The adsorption of HPOs to the lipid monolayers was followed by the increase of surface pressure as described previously [16,17]. As control experiment, the same volume of pure DMSO was injected underneath the lipid monolayer and no change of the surface pressure was observed. The maximal insertion pressure is defined as the initial surface pressure for which the injection of HPOs did not induce any surface pressure increase of the monolayer. The maximal insertion surface pressure (MIP) was obtained by linear regression of the plot $\Delta\Pi$ vs Π_i. The "differential Π_0 ($d\Pi_0$)" parameter was calculated as follows:

$$d\Pi_0 = \Delta\Pi_0 - \Pi_e$$

where $\Delta\Pi_0$ corresponds to the y-intercept of the linear regression of the $\Delta\Pi$ vs Π_i plot, and Π_e is the surface pressure increase at the equilibrium obtained in an independent experiment performed at the same HPO concentration but without lipids spread at the interface.

The uncertainty in the MIP and in the $d\Pi_0$ were calculated as described previously [18–21].

2.4. Preparation of liposomes

2.4.1. Preparation of multilamellar vesicles

Multilamellar vesicles (MLVs) were prepared as described in [16,22]. Pure PLPC or PLPC with sitosterol (PLPC/sitosterol, 70/30 molar ratio) or PLPC with GluCer (70/30, molar ratio) were dissolved in a chloroform/methanol mixture (2/1, v/v) alone or in the presence of HPOs at a molar ratio lipid/HPOs 20/1. The chloroform/methanol mixture was evaporated to obtain a lipid film dried under vacuum overnight. The resulting film was hydrated by deuterium oxide above

the phase transition temperature of lipids. The hydrated film was vortexed continuously to obtain MLVs.

2.4.2. Preparation of large unilamellar vesicles

Large unilamellar vesicles (LUVs) were prepared as described previously [16,23]. Lipid films were prepared in the same manner than MLVs and were then hydrated above the transition temperature of lipids during 1h at 40°C and shaken every 10 min. 5 cycles of freeze-thawing were applied to the spontaneously formed multilamellar vesicles. To obtain LUVs, this suspension was sonicated to clarity (5 cycles x 2min) using a probe with 400 W amplitude keeping the suspension in an ice bath. At the end, titanium particles were removed from LUV solution by centrifuging during 10 min at 2000 g.

2.5. Infrared spectroscopy (FT-IR)

Infrared spectra were measured using a Bruker Equinox 55 spectrometer (Karlsruhe, Germany) equipped with a liquid nitrogen-cooled Mercury–Cadmium-Telluride detector and linked to a computer with OPUS software (Bruker). The number of scans was 128 at 4 cm^{-1} resolution. During all measurements, the spectrometer was continuously purged with N_2 flux. All the experiments were performed with a demountable cell (Bruker) equipped with CaF2 windows. Each spectrum is the representative of at least two independent measurements.

2.6. Isothermal titration calorimetry measurements

ITC experiments were performed as described previously [16]. All measurements were performed using a VP-ITC (MicroCal, Northampton, MA). Before starting the experiments, solutions were degassed by stirring under vacuum or by ultrasonication. The sample cell was filled out with Tris HCl buffer at pH 7.4 (blank) or a HPO solution at 10 µM (below CMC) in Tris HCl buffer at pH 7.4 and the reference cell was loaded with milli-Q water. The volume of

sample cell was 1.4565 ml. Titration experiments were done with a 300 µL-syringe containing lipid LUV suspension at 2 mM in Tris HCl buffer at pH 7.4 at 25 °C. The sample cell was stirred continuously at 305 rpm during experiments. A titration experiment was performed by consecutive injections of 10 µL of LUV into the HPOs solution. Each injection took 14.5 sec and a delay of 200 sec between injections was applied in order to reach a steady state before each new injection. The effective heats were determined by subtracting the values obtained for the blanks from the observed heats. Raw data were processed using the software provided by the manufacturer (ORIGIN 7 – Originlab, Northampton, USA). The ITC data were treated according to the cumulative model described previously [24] and previously applied for other types of surfactants [25,26]. The thermodynamic parameters were calculated as described in [24]. Calculations provided the values of the molar free energy (ΔG), the molar enthalpy change (ΔH) and the molar entropy change ($T\Delta S$) of the binding reactions as well as the binding coefficient (K) related to the affinity of HPOs for LUVs.

2.7. *In silico* approaches

2.7.1. Hypermatrix docking method

A simple docking method called Hypermatrix described elsewhere [23,27,28] was used in order to dock HPOs to different lipid systems, as recently done for saponins [29]. Briefly, the HPO molecule is put in a fixed position at the center of system and oriented at the hydrophobic/hydrophilic interface and the lipid molecule, also oriented at the lipid/water interface, is positioned around the HPO molecule by rotations and translations (more than 10^7 positions tested). For each position, an energy value is calculated, according to an empirical forcefield [30]. The energy values together with the coordinates of all assemblies are stored in a matrix and classified according to decreasing values. The most stable matching is used to decide the position of the first lipid. The position of the second lipid is then defined as the next most energetically favorable orientation stored in the matrix taking steric and energetic

constraints due to the presence of the first lipid molecule into account. The process is completed when the central molecule is completely surrounded with lipids [23,27,28]. The structure of HPOs correspond to the structure obtained after molecular dynamics (see point 2,7,3).

2.7.2. Big monolayer method

The big monolayer method was used as described [23,29,31]. First, paired interactions between molecules are calculated according to the docking method (see above) and secondly a grid of 200x200 molecules is constructed taking the molar ratios used experimentally into account. In this study, these pairs were HPOD/PLPC, HPOD/sito, HPOD/GluCer, HPOT/PLPC, HPOT/sito, HPOT/GluCer, PLPC/sito, PLPC/GluCer and sito/GluCer. For each pair of molecules, a Bolzmann energy is calculated by adding the interaction energy of each relative position tested multiplied by the probability of the position. Then, a grid of 40,000 (200×200) molecules, initially positioned at random, is constructed and the energy of the system is calculated. Random permutations are made, and the energy of the new configuration is calculated. The whole system is minimized by a Monte Carlo procedure performing 100.000 steps. Three repetitions of each system were calculated. Each molecule is represented by a pixel, generating an image of the molecular domains formed.

2.7.3. Molecular dynamics

HPOD and HPOT have been studied by molecular dynamics (MD) in presence of a membrane of PLPC, PLPC/Sitosterol (70/30), PLPC/GluCer (70/30) or PLPC/Sitosterol/GluCer (60/20/20). Their topologies for the Gromos 53a6 force field [32] have been generated by using the Automated Topology Builder server "http://compbio.chemistry.uq.edu.au/atb/" [33–35]. The membranes (288 molecules) have been generated at a coarse grained resolution suitable for the MARTINI forcefield [36] by using Insane [37]. A 5,000 steps of steepest-descent energy minimization was performed to remove

any steric clashes and production simulations have been run for 100 ns. Temperature and pressure were coupled at 303 K and 1 bar using the weak coupling Berendsen algorithm with $\tau T = 1$ ps and $\tau P = 1$ ps [38]. Pressure was coupled semiisotropically. Non-bonded interactions were computed up to 1.2 nm with the shift method. Electrostatics were treated with $\varepsilon = 15$. The compressibility was 3×10^4 (1/bar).

The membrane systems have been converted to an atomistic representation suitable for the Gromos 53a6 force field using Backwards [39]. HPOD and HPOT were placed at 1 nm from the membrane and the box filled with SPC water [40]. All the systems studied were first minimized by steepest descent for 5,000 steps. 100 ps NVT and 1 ns NPT simulations with the peptides under position restraints were run before production simulations were performed. Periodic boundary conditions (PBC) are used with a 2 fs time step. The dynamics were carried out at 303 K and 1 bar for 500 ns. After this simulation, HPOs have been translated in the XY plane to generate a membrane with 20 HPOs. 100 ps NVT and 1 ns NPT simulations with the peptides under position restraints were run before production simulations of 1µs were performed. Temperature was maintained by using the v-rescale method [41,42] with $\tau T = 0.5$ ps and an semi-isotropic pressure was maintained by using the Parrinello-Rahman barostat [43] with a compressibility of 4.6 × 10^5 (1/bar) and $\tau P = 2$ ps. Electrostatic interactions were treated by using the particle mesh Ewald (PME) method [44]. Van der Waals and electrostatics were treated with a 1.0 nm cut-off. Bond lengths were maintained with the LINCS algorithm [45]. Trajectories were performed and analyzed with GROMACS 5.0.7 tools. MDAnalysis has also been used [46]. 3D structures were analyzed with both PYMOL [47] and VMD [48] softwares.

3. Results and discussion

3.1. Interaction of HPOs with PPM-mimicking models

The first objective of this study was to determine the ability of HPO to interact with PPM. Complex liposomes mimicking PPM composed of palmitoyl linoleoyl phosphatidylcholine (PLPC) as model phospholipid, sitosterol as model sterol and glucosylceramide (GluCer) as model sphingolipid were prepared [23]. The thermodynamic profile (Figure S2) and parameters (Figure S3) of the binding of both HPOs with these liposomes were determined by isothermal titration calorimetry. The binding profiles of HPOT or HPOD show negative peaks with an area decreasing gradually with the successive liposome injections. The rate of decrease is much higher for HPOT than HPOD.

For both HPOs, their binding reaction to complex liposomes mimicking PPM, was spontaneous ($\Delta G < 0$), exothermic ($\Delta H < 0$) and generated a positive change of entropy ($\Delta S > 0$). These data demonstrate that both molecules can bind to liposomes, suggesting an interaction with the lipid phase of the PPM. The absolute values of entropy change are higher than the absolute values of enthalpy change indicating that the binding is notably driven by hydrophobic interactions [49]. The binding coefficient (K) and ΔH are significantly different for HPOT and HPOD, showing a higher affinity of HPOT compared to HPOD for the complex liposomes.

Molecular dynamics was performed to visualize the insertion of HPOs in a ternary model of plant plasma bilayer at an atomistic scale. Each molecule inserts into the membrane in few nanoseconds when they are outside the membrane in a coarse-grained representation (Figure 2), suggesting significant affinity for plant lipids, in agreement with the above experimental assays. After insertion, both HPOs adopt a conformation with their acid group in contact with lipid choline groups and water, the peroxide at the level of glycerol and the double bonds in the hydrophobic core, mainly parallel to the membrane. The distance of characteristic

moieties from the membrane center is as follows: COO- > OOH > carbon of the first double bond > CH_3.

The simulation of the lateral distribution of HPOs within the ternary model membrane was obtained by the modeling method Big Monolayer (BM) (Figure 3).

In the absence of HPOs, GluCer-sitosterol enriched domains are generated within the PLPC matrix in quite accordance with previous molecular dynamics study [50]. The presence of each HPO influences very differently the lateral reorganization of the domains. In presence of HPOT, bigger GluCer domains comprising some HPOT and a very few sitosterol are formed in the PLPC matrix besides smaller dissociated domains of sitosterol containing also HPOT molecules. In contrast, the addition of HPOD results into the dissociation of sitosterol clusters and their regular distribution around the similar size GluCer patches containing the majority of HPOD.

3.2. Lipid specificity of the HPO-model membrane interactions

Since HPOs are able to interact with the complex liposomes, the next question is to determine if there is any lipid specificity for this interaction. To address this question, liposomes containing pure PLPC, PLPC/sitosterol or PLPC/GluCer were prepared and the thermodynamic parameters for the binding of both HPOs with these different liposomes were determined (Figure 4).

Regardless the composition of the liposomes, the binding reactions are spontaneous ($\Delta G<0$), exothermic ($\Delta H<0$) and generate a large positive change of entropy ($T\Delta S>0$). As for complex liposomes, hydrophobic interactions are the predominant component in the binding of both HPOs to liposomes. For each lipid system, the binding coefficients are higher for HPOT compared to HPOD, confirming a higher affinity of HPOT for lipids. Concerning the lipid specificity, the presence of sitosterol decreases the binding coefficients and the enthalpy values for HPOT and to a lesser extent for HPOD comparatively to pure PLPC and binary PLPC/GluCer compositions. The negative influence of sitosterol is strengthened by the

presence of GluCer seeing that the binding coefficients and ΔH values are lower for the ternary system (Figure S3) compared to the binary ones (Figure 4).

Since it is not possible to prepare liposomes containing only sitosterol or GluCer, the interactions energies with individual lipid were calculated using the hypermatrix docking method (Figure S4). The absolute values of the interaction energies were in the order GluCer>PLPC>sitosterol for both HPOs, confirming the less favorable interaction of HPOs with sitosterol molecules.

To determine if the first step of insertion plays a role in this lipid specificity, adsorption into individual lipid monolayer was analyzed. The adsorption was monitored by the increase of the surface pressure at a constant trough area (Figure S5).

For an initial surface pressure between 5 and 10 mN/m, the adsorption kinetics of HPOT and HPOD into PLPC or sitosterol monolayers were not significantly different while in the case of GluCer or lipid ternary mixture monolayers, HPOT displays a faster adsorption kinetic than HPOD (Figure S5).

The plots of the maximal surface pressure variation (ΔΠ) versus the initial surface pressure (Πi) obtained for the individual lipid monolayers and the ternary composition monolayer, and the corresponding binding parameters are shown in Figure S6, and Figure 5A and B respectively.

For all the compositions, ΔΠ decreases linearly with increasing values of Πi, indicating that a higher packing of lipid molecules at the air−water interface leads to a weaker adsorption of the HPOs into the monolayer, as generally observed for other amphiphilic molecules [16,17,23].

The maximal insertion pressure (MIP) value which reflects the penetration power of HPOs into lipid monolayer, shows, in the case of the ternary composition, values higher than the lateral pressure supposed to prevail within biological membranes (30-35 mN/m) [51], suggesting that HPOs can insert into natural PPM. The positive values of dΠ0 values confirm an attractive effect of PPM mimicking lipids on the HPOs adsorption. The effect is higher for HPOT than

HPOD in terms of penetration power as well as in terms of attractivity for the ternary composition.

Individual lipids do not shown the same trends as observed for the ternary lipid mixture, especially in terms of attractivity. Each lipid exerts a higher attractive effect on HPOD compared to HPOT. It suggests that the lateral arrangement of the whole lipids within the membrane exerts an important effect on the insertion of the HPOs.

Differently to what it is observed by ITC, sitosterol does not show a less favorable effect on the HPOs adsorption comparatively to PLPC and GluCer. In the adsorption experiments, the lipid model is a monolayer while it is a bilayer in the ITC experiments. Moreover the liposome model is composed of a binary mixture of PLPC and sitosterol while in monolayer ones, it is sitosterol alone. The presence of a second sheet and the ordering effect of sitosterol on the PC membrane [52] have undoubtedly an influence on the insertion behavior of the HPOs.

3.3. Molecular features of lipid-HPO's interactions

The lipid chemical groups involved in the interaction were determined by FTIR spectroscopy by comparing the spectra of liposomes with or without HPOs. Pure PLPC liposomes and PLPC/sitosterol or PLPC/GluCer binary mixture liposomes were used.

In the 3000-2800 cm^{-1} region , the spectrum of pure PLPC shows three bands located at 2956 cm^{-1}, 2923.5 cm^{-1} and 2854 cm^{-1} corresponding to the CH_3 stretching, CH_2 asymmetric stretching and CH_2 symmetric stretching of the alkyl chain, respectively [23,53]. In presence of HPOs, a slight but significant shift [54,55] to lower wavenumbers is observed for the three bands (Figure S7A and Table 1). It indicates a more rigid state for PLPC alkyl chains in the presence of HPOs [56,57], HPOD and HPOT inducing the same effect.

No significant influence of HPOT or HPOD is observed in the C=O ester region (band at 1732 cm^{-1}) (Figure S7B and Table 1). Interestingly, a significant difference between HPOD and HPOT is noticed in the phosphate region (Figure S7C and Table 1). The band at 1226 cm^{-1}

corresponding to the asymmetric stretching of the phosphate group [58,59] shifts slightly to higher wavenumbers (1228 cm^{-1}) in the presence of HPOD while the presence of HPOT considerably shifts the band to lower wavenumbers (1218 cm^{-1}). Shifts in the phosphoryl stretching are interpreted in terms of hydrogen bonding which can be related to the degree of hydration of the phosphate group [60]. For HPOT, the shift to lower wavenumbers indicates a more hydrogen-bonded state of the phosphate groups while in the case of HPOD, the slight shift to higher wavenumbers indicates a less hydrogen-bonded state of the phosphate groups. Nonetheless, an effect on the orientation of the phosphate headgroups with respect to the bilayer plane cannot be ruled out and could be analyzed with polarized IR. These effects could be due to a direct interaction between the PLPC phosphate groups with the polar heads of HPOs and/or to an indirect influence of the presence of HPOs on the arrangement of polar headgroups of the phospholipids.

These results obviously reveal that the interactions of HPOT and HPOD with PLPC molecules are quite different from a molecular point of view.

The presence of sitosterol in the lipid system does not induce any modification of the alkyl chains neither for the phosphate group, nor for the C=O ester group when HPOT is present. In the case of HPOD, a shift to lower wavenumbers is only observed for the phosphate group band, in contrast to what happens when PLPC is alone (Table 1). By ordering the phospholipid molecules [61], sitosterol could hinder the interactions between the polar parts of PLPC and HPOs.

Addition of HPOs on the GluCer-containing system leads to a shift of the CH_2 asymmetric and symmetric stretching bands to higher wavenumbers indicating a fluidizing effect. The influence of HPOs on the phosphate group vibrations and on the C=O ester group in presence of GluCer is the same as the one observed for PLPC alone.

Molecular dynamics performed on PLPC, PLPC/sitosterol, PLPC/GluCer and PLPC/sitosterol/GluCer show that the interactions of HPOs with the membrane change when sitosterol or GluCer or sitosterol/GluCer are added. HPOs and particularly HPOD are less deeply inserted (Figure 6) and there are less salt bridges formed between HPO acid groups and PLPC choline group (from 63 for PLPC alone to 52, 49 and 50 in average for 20 HPOD in PLPC/sitosterol, PLPC/GluCer and PLPC/sitosterol/GluCer, respectively). Instead, HPOs are forming more hydrogen bonds with water and GluCer, mainly between the acid group and the glucosyl part. In the case of HPOD, the angle between the HPO double bonds and the membrane normal is also influenced by the presence of sitosterol or GluCer or sitosterol/GluCer mixture. In PLPC, the double bonds are almost parallel to the bilayer surface. When sitosterol or/and GluCer are added, the angle tends to decrease, the carbon linked to the hydroperoxide (C2) going at lower position than the one at the beginning of the double bonds (C1) (Figure 6B). Differently, the angle for HPOT is not significantly influenced by the nature of the lipid and its value is in average higher than for HPOD.

The differential insertion and interaction properties between HPOT and HPOD could hence be explained by their respective orientation within the membrane. HPOT having a supplementary double bond blocking its torsional angle has a more shaped conformation while HPOD has more freedom on its acyl chain. Taking all together, these results suggest the modulation of the lipid interactions of both HPOs by the presence of a double bond. Accordingly, we have previously shown that a supplementary double bound could induce modulation of membrane interaction properties of sugar bolaamphiphiles [62].

4. General discussion and conclusion

Key intermediate oxylipins, HPOD and HPOT, play an important role during the plant lifecycle [63,64], especially in plant defense against pathogens by direct antimicrobial action [12]. Even though numerous studies have been carried out to understand the HPOs biosynthesis and their conversion into molecules with different physiological features, there is no study addressing the traffic of HPOs at a subcellular scale during pathogen attack. How they come into contact with the phytopathogens, whether they are released into the apoplastic medium, are still open questions. One hypothesis is that they are excreted by the plant cells through the plasma membrane. As their structure is amphiphile they can also be supposed to interact with plasma membrane lipids and play a role in the defense mechanism at this place.

The *in silico* and *in vitro* experiments conducted in the present study clearly demonstrate that HPOs are able to interact with PPM lipids and to perturb their lateral organization. Even though both HPOs are able to interact with phospholipids, sterols and sphingolipids, GluCer seems to be a privileged partner while sitosterol has a less favored interaction. Moreover, the physical state and nanolateral organization of the membrane has a strong influence on their interaction. The presence of sitosterol known to order phospholipid bilayers [52] reduces the binding of HPOs. We also suggest that the interplay of sitosterol with GluCer forming intricate clusters separated from the PLPC matrix further reduces the propensity of HPOs to interact but does not annihilate it. Of course, other lipids (such as campesterol, stigmasterol and conjugated sterols in the sterol class, matched chain and saturated phospholipids and glycosylinositolphosphoceramides in the sphingolipid category) are present in natural PPMs and could be of importance for the interaction of HPO with plant cells.

The binding of HPO to liposomes is globally dominated by hydrophobic interactions. However, molecular details of the interaction analyzed by FTIR and MD approach showed that polar interactions are also involved. The hydrogen bonding state of phosphate groups of PLPC as

well as the amide groups of GluCer are modified. MD simulations show accordingly interactions between the lipid polar parts and HPOs.

The chemical structure of HPOs plays an important role in the interactions. Globally, HPOT, comprising three double bonds, has more affinity for model bilayers compared to HPOD containing two double bonds. The interactions at the level of lipid polar parts seem to be determinant for the differential effects of HPOT and HPOD, due to a stiffening of the acyl chain of HPOT. Our results suggest that HPOT creates more interactions with the lipid polar parts through both its acid and hydroperoxide groups than HPOD.

Lipid specificity of the HPO-membrane interactions as well as the differences observed between HPOT and HPOD could also play an important role in plant cell signaling. By modifying the plasma membrane lateral organization, they could participate to the recruitment of key proteins in the signaling cascade of plant defense. This hypothesis is under investigation by our group.

Acknowledgements

M.N.N. and JMC have been working for the ARC-FIELD project. E.D. is supported by the "Formation à la Recherche dans l'Industrie et l'Agriculture" (FRIA) grant from the F.R.S.-F.N.R.S. M.D., MO and L.L. thank the F.R.S.-F.N.R.S. (National Funds for Scientific Research, Belgium) for their positions as Senior Research Associates. The authors thank also the financial support via the project from University of Liège (ARC-FIELD project 13/17-10) and ED thanks the FRIA for the FC20989 grant, and MD and LL thank the FRS FNRS for the PDR T.1003.14 grant and their respective CDR grants (CDR J.0086.18 and CDR J.0114.18) . Partial computational resources of the lab are provided by the "Consortium des Équipements de Calcul Intensif" (CÉCI), funded by the F.R.S.-FNRS under Grant No. 2.5020.11. The authors also thank the HPC-Regional Center ROMEO (https://romeo.univ-reims.fr) and the Multiscale Molecular Modeling Platform (P3M: https://p3m.univ-reims.fr) from the University of Reims Champagne-Ardenne (France) for providing CPU time and support.

References

[1] R.A. Creelman, R. Mulpuri, The Oxylipin Pathway in Arabidopsis, Arab. B. 1 (2002) e0012. doi:10.1199/tab.0012.

[2] E. Blée, Impact of phyto-oxylipins in plant defense, Trends Plant Sci. 7 (2002) 315–321. doi:10.1016/S1360-1385(02)02290-2.

[3] M. Mariutto, F. Duby, A. Adam, C. Bureau, M.L. Fauconnier, M. Ongena, P. Thonart, J. Dommes, The elicitation of a systemic resistance by Pseudomonas putida BTP1 in tomato involves the stimulation of two lipoxygenase isoforms, BMC Plant Biol. 11 (2011) 29. doi:10.1186/1471-2229-11-29.

[4] A. Mosblech, I. Feussner, I. Heilmann, Oxylipins: Structurally diverse metabolites from fatty acid oxidation, Plant Physiol. Biochem. 47 (2009) 511–517. doi:10.1016/j.plaphy.2008.12.011.

[5] V. Gosset, N. Harmel, C. Gobel, F. Francis, E. Haubruge, J.-P. Wathelet, P. du Jardin, I. Feussner, M.-L. Fauconnier, Attacks by a piercing-sucking insect (Myzus persicae Sultzer) or a chewing insect (Leptinotarsa decemlineata Say) on potato plants (Solanum tuberosum L.) induce differential changes in volatile compound release and oxylipin synthesis, J. Exp. Bot. 60 (2009) 1231–1240. doi:10.1093/jxb/erp015.

[6] L.M. Babenko, M.M. Shcherbatiuk, T.D. Skaterna, I. V Kosakivska, Lipoxygenases and their metabolites in formation of plant stress tolerance., Ukr. Biochem. J. 89 (n.d.) 5–21. http://www.ncbi.nlm.nih.gov/pubmed/29236385 (accessed July 25, 2018).

[7] H. Porta, Plant Lipoxygenases. Physiological and Molecular Features, PLANT Physiol. 130 (2002) 15–21. doi:10.1104/pp.010787.

[8] A. Mosblech, I. Feussner, I. Heilmann, Lipid Signaling in Plants, 2010. doi:10.1007/978-3-642-03873-0.

[9] A. Andreou, I. Feussner, Lipoxygenases - Structure and reaction mechanism, Phytochemistry. 70 (2009) 1504–1510. doi:10.1016/j.phytochem.2009.05.008.

[10] C. Schneider, D.A. Pratt, N.A. Porter, A.R. Brash, Control of Oxygenation in Lipoxygenase and Cyclooxygenase Catalysis, Chem. Biol. 14 (2007) 473–488. doi:10.1016/j.chembiol.2007.04.007.

[11] G.A. Howe, A.L. Schilmiller, Oxylipin metabolism in response to stress, Curr Opin Plant Biol. 5 (2002) 230–236. doi:S1369526602002509 [pii].

[12] I. Prost, Evaluation of the Antimicrobial Activities of Plant Oxylipins Supports Their Involvement in Defense against Pathogens, PLANT Physiol. (2005). doi:10.1104/pp.105.066274.

[13] G. Granér, M. Hamberg, J. Meijer, Screening of oxylipins for control of oilseed rape (Brassica napus) fungal pathogens, Phytochemistry. (2003). doi:10.1016/S0031-9422(02)00724-0.

[14] H. Tran Thanh, L. Beney, H. Simonin, T.X.S. Nguyen, P. Gervais, J.M. Belin, F. Husson, Toxicity of fatty acid hydroperoxides towards Yarrowia lipolytica: Implication of their membrane fluidizing action, Biochim. Biophys. Acta - Biomembr. (2007). doi:10.1016/j.bbamem.2007.05.016.

[15] M.L. Fauconnier, M. Marlier, An efficient procedure for the production of fatty acid hydroperoxides from hydrolyzed flax seed oil and soybean lipoxygenase, Biotechnol. Tech. 10 (1996) 839–844. doi:10.1007/BF00154668.

[16] M.N. Nasir, J.M. Crowet, L. Lins, F. Obounou Akong, A. Haudrechy, S. Bouquillon, M. Deleu, Interactions of sugar-based bolaamphiphiles with biomimetic systems of plasma membranes, Biochimie. (2016). doi:10.1016/j.biochi.2016.04.001.

[17] M.N. Nasir, F. Besson, Conformational analyses of bacillomycin D, a natural

antimicrobial lipopeptide, alone or in interaction with lipid monolayers at the air–water interface, J. Colloid Interface Sci. 387 (2012) 187–193. doi:10.1016/j.jcis.2012.07.091.
[18] P. Calvez, S. Bussières, Éric Demers, C. Salesse, Parameters modulating the maximum insertion pressure of proteins and peptides in lipid monolayers, Biochimie. (2009). doi:10.1016/j.biochi.2009.03.018.
[19] P. Calvez, E. Demers, E. Boisselier, C. Salesse, Analysis of the contribution of saturated and polyunsaturated phospholipid monolayers to the binding of proteins, Langmuir. (2011). doi:10.1021/la104097n.
[20] M.N. Nasir, F.F. Besson, Specific Interactions of Mycosubtilin with Cholesterol-Containing Artificial Membranes., Langmuir. 27 (2011) 10785–10792. doi:10.1021/la200767e.
[21] M.N. Nasir, L. Lins, J.-M. Crowet, M. Ongena, S. Dorey, S. Dhondt-Cordelier, C. Clément, S. Bouquillon, A. Haudrechy, C. Sarazin, M.-L. Fauconnier, K. Nott, M. Deleu, Differential Interaction of Synthetic Glycolipids with Biomimetic Plasma Membrane Lipids Correlates with the Plant Biological Response, Langmuir. 33 (2017). doi:10.1021/acs.langmuir.7b01264.
[22] A. Kouzayha, M.N. Nasir, R. Buchet, O. Wattraint, C. Sarazin, F. Besson, Conformational and interfacial analyses of K3A18K3 and alamethicin in model membranes., J. Phys. Chem. B. 113 (2009) 7012–9. doi:10.1021/jp810539b.
[23] M. Deleu, J.-M.M. Crowet, M.N. Nasir, L. Lins, Complementary biophysical tools to investigate lipid specificity in the interaction between bioactive molecules and the plasma membrane: A review., Biochim. Biophys. Acta. 1838 (2014) 3171–3190. doi:10.1016/j.bbamem.2014.08.023.
[24] H. Heerklotz, J. Seelig, Titration calorimetry of surfactant–membrane partitioning and membrane solubilization, Biochim. Biophys. Acta - Biomembr. 1508 (2000) 69–85. doi:10.1016/S0304-4157(00)00009-5.
[25] F.N. Zakanda, L. Lins, K. Nott, M. Paquot, G.M. Lelo, M. Deleu, Interaction of hexadecylbetainate chloride with biological relevant lipids, Langmuir. (2012). doi:10.1021/la2040328.
[26] H. Razafindralambo, S. Dufour, M. Paquot, M. Deleu, Thermodynamic studies of the binding interactions of surfactin analogues to lipid vesicles, J. Therm. Anal. Calorim. (2009). doi:10.1007/s10973-008-9403-6.
[27] O. Bouffioux, A. Berquand, M. Eeman, M. Paquot, Y.F. Dufrêne, R. Brasseur, M. Deleu, Molecular organization of surfactin-phospholipid monolayers: effect of phospholipid chain length and polar head., Biochim. Biophys. Acta. 1768 (2007) 1758–68. doi:10.1016/j.bbamem.2007.04.015.
[28] R. Brasseur, M. Vandenbranden, B. Cornet, A. Burny, J.M. Ruysschaert, Orientation into the lipid bilayer of an asymmetric amphipathic helical peptide located at the N-terminus of viral fusion proteins, BBA - Biomembr. (1990). doi:10.1016/0005-2736(90)90163-I.
[29] E.J.S. Claereboudt, I. Eeckhaut, L. Lins, M. Deleu, How different sterols contribute to saponin tolerant plasma membranes in sea cucumbers, Sci. Rep. 8 (2018) 10845. doi:10.1038/s41598-018-29223-x.
[30] L. Lins, R. Brasseur, The hydrophobic effect in protein folding., FASEB J. 9 (1995) 535–40. doi:10.1042/BJ20100615.
[31] M. Deleu, J. Lorent, L. Lins, R. Brasseur, N. Braun, K. El Kirat, T. Nylander, Y.F. Dufrêne, M.-P. Mingeot-Leclercq, Effects of surfactin on membrane models displaying lipid phase separation., Biochim. Biophys. Acta. 1828 (2013) 801–15. doi:10.1016/j.bbamem.2012.11.007.
[32] C. Oostenbrink, A. Villa, A.E. Mark, W.F. Van Gunsteren, A biomolecular force field

based on the free enthalpy of hydration and solvation: The GROMOS force-field parameter sets 53A5 and 53A6, J. Comput. Chem. (2004). doi:10.1002/jcc.20090.

[33] A.K. Malde, L. Zuo, M. Breeze, M. Stroet, D. Poger, P.C. Nair, C. Oostenbrink, A.E. Mark, An Automated force field Topology Builder (ATB) and repository: Version 1.0, J. Chem. Theory Comput. (2011). doi:10.1021/ct200196m.

[34] S. Canzar, M. El-Kebir, R. Pool, K. Elbassioni, A.K. Malde, A.E. Mark, D.P. Geerke, L. Stougie, G.W. Klau, Charge Group Partitioning in Biomolecular Simulation, J. Comput. Biol. 20 (2013) 188–198. doi:10.1089/cmb.2012.0239.

[35] K.B. Koziara, M. Stroet, A.K. Malde, A.E. Mark, Testing and validation of the Automated Topology Builder (ATB) version 2.0: prediction of hydration free enthalpies., J. Comput. Aided. Mol. Des. 28 (2014) 221–33. doi:10.1007/s10822-014-9713-7.

[36] S.J. Marrink, H.J. Risselada, S. Yefimov, D.P. Tieleman, A.H. De Vries, The MARTINI force field: Coarse grained model for biomolecular simulations, J. Phys. Chem. B. 111 (2007) 7812–7824. doi:10.1021/jp071097f.

[37] T.A. Wassenaar, H.I. Ingólfsson, R.A. Böckmann, D.P. Tieleman, S.J. Marrink, Computational Lipidomics with *insane* : A Versatile Tool for Generating Custom Membranes for Molecular Simulations, J. Chem. Theory Comput. 11 (2015) 2144–2155. doi:10.1021/acs.jctc.5b00209.

[38] H.J.C. Berendsen, J.P.M. Postma, W.F. van Gunsteren, A. DiNola, J.R. Haak, Molecular dynamics with coupling to an external bath, J. Chem. Phys. 81 (1984) 3684–3690. doi:10.1063/1.448118.

[39] T.A. Wassenaar, K. Pluhackova, R.A. Böckmann, S.J. Marrink, D.P. Tieleman, Going backward: A flexible geometric approach to reverse transformation from coarse grained to atomistic models, J. Chem. Theory Comput. (2013) 131220152755007. doi:10.1021/ct400617g.

[40] H.J.C. Berendsen, J.P.M. Postma, W.F. van Gunsteren, J. Hermans, Interaction Models for Water in Relation to Protein Hydration, in: Springer, Dordrecht, 1981: pp. 331–342. doi:10.1007/978-94-015-7658-1_21.

[41] G. Bussi, D. Donadio, M. Parrinello, Canonical sampling through velocity rescaling, J. Chem. Phys. 126 (2007) 014101. doi:10.1063/1.2408420.

[42] S. Nosé, A molecular dynamics method for simulations in the canonical ensemble, Mol. Phys. 52 (1984) 255–268. doi:10.1080/00268978400101201.

[43] M. Parrinello, Polymorphic transitions in single crystals: A new molecular dynamics method, J. Appl. Phys. 52 (1981) 7182. doi:10.1063/1.328693.

[44] U. Essmann, L. Perera, M.L. Berkowitz, T. Darden, H. Lee, L.G. Pedersen, A smooth particle mesh Ewald method, J. Chem. Phys. 103 (1995) 8577. doi:10.1063/1.470117.

[45] B. Hess, H. Bekker, H.J.C. Berendsen, J.G.E.M. Fraaije, LINCS: A linear constraint solver for molecular simulations, J. Comput. Chem. 18 (1997) 1463–1472. doi:10.1002/(SICI)1096-987X(199709)18:12<1463::AID-JCC4>3.0.CO;2-H.

[46] N. Michaud-Agrawal, E.J. Denning, T.B. Woolf, O. Beckstein, MDAnalysis: A toolkit for the analysis of molecular dynamics simulations, J. Comput. Chem. 32 (2011) 2319–2327. doi:10.1002/jcc.21787.

[47] L. Schrödinger, The PyMOL Molecular Graphics System, Version 1.3, (2010).

[48] W. Humphrey, A. Dalke, K. Schulten, VMD: visual molecular dynamics., J. Mol. Graph. 14 (1996) 33–8, 27–8.

[49] K. Bouchemal, New challenges for pharmaceutical formulations and drug delivery systems characterization using isothermal titration calorimetry, Drug Discov. Today. 13 (2008) 960–972. doi:10.1016/j.drudis.2008.06.004.

[50] S. Emami, S. Azadmard-Damirchi, S.H. Peighambardoust, J. Hesari, H. Valizadeh, R.

Faller, Molecular dynamics simulations of ternary lipid bilayers containing plant sterol and glucosylceramide, Chem. Phys. Lipids. 203 (2017) 24–32. doi:10.1016/J.CHEMPHYSLIP.2017.01.003.

[51] D. Marsh, Lateral pressure in membranes, Biochim. Biophys. Acta - Rev. Biomembr. 1286 (1996) 183–223. doi:10.1016/S0304-4157(96)00009-3.

[52] K. Grosjean, S. Mongrand, L. Beney, F. Simon-Plas, P. Gerbeau-Pissot, Differential effect of plant lipids on membrane organization: specificities of phytosphingolipids and phytosterols., J. Biol. Chem. 290 (2015) 5810–25. doi:10.1074/jbc.M114.598805.

[53] L. Ter-Minassian-Saraga, E. Okamura, J. Umemura, T. Takenaka, Fourier transform infrared-attenuated total reflection spectroscopy of hydration of dimyristoylphosphatidylcholine multibilayers, Biochim. Biophys. Acta - Biomembr. 946 (1988) 417–423. doi:10.1016/0005-2736(88)90417-8.

[54] V.R. Kodati, M. Lafleur, Comparison between orientational and conformational orders in fluid lipid bilayers., Biophys. J. 64 (1993) 163–70. doi:10.1016/S0006-3495(93)81351-1.

[55] W. Pohle, D.R. Gauger, U. Dornberger, E. Birch-Hirschfeld, C. Selle, A. Rupprecht, M. Bohl, Hydration of biological molecules: Lipids versus nucleic acids, Biopolymers. 67 (2002) 499–503. doi:10.1002/bip.10164.

[56] W. Pohle, C. Selle, H. Fritzsche, H. Binder, Fourier Transform Infrared Spectroscopy as a Probe for the Study of the Hydration of Lipid Self-Assemblies . I ., (1998) 267–280.

[57] L.K. Tamm, S.A. Tatulian, Infrared spectroscopy of proteins and peptides in lipid bilayers., Q. Rev. Biophys. 30 (1997) 365–429. http://journals.cambridge.org/abstract_S0033583597003375 (accessed March 13, 2014).

[58] M.N. Nasir, A. Thawani, A. Kouzayha, F. Besson, Interactions of the natural antimicrobial mycosubtilin with phospholipid membrane models., Colloids Surf. B. Biointerfaces. 78 (2010) 17–23. doi:10.1016/j.colsurfb.2010.01.034.

[59] J.L.R. Arrondo, F.M. Goñi, Protein-Lipid Interactions, Elsevier, 1993. doi:10.1016/S0167-7306(08)60242-2.

[60] F.M. Goñi, J.L.R. Arrondo, A study of phospholipid phosphate groups in model membranes by Fourier transform infrared spectroscopy, Faraday Discuss. Chem. Soc. 81 (1986) 117–126. doi:10.1039/DC9868100117.

[61] K. Grosjean, S. Mongrand, L. Beney, F. Simon-Plas, P. Gerbeau-Pissot, Differential Effect of Plant Lipids on Membrane Organization, J. Biol. Chem. 290 (2015) 5810–5825. doi:10.1074/jbc.M114.598805.

[62] M. Deleu, S. Gatard, E. Payen, L. Lins, K. Nott, C. Flore, R. Thomas, M. Paquot, S. Bouquillon, d-xylose-based bolaamphiphiles: Synthesis and influence of the spacer nature on their interfacial and membrane properties, Comptes Rendus Chim. 15 (2012) 68–74. doi:10.1016/J.CRCI.2011.10.006.

[63] C. Wasternack, Jasmonates: An Update on Biosynthesis, Signal Transduction and Action in Plant Stress Response, Growth and Development, Ann. Bot. 100 (2007) 681–697. doi:10.1093/aob/mcm079.

[64] G. Griffiths, Biosynthesis and analysis of plant oxylipins, Free Radic. Res. 49 (2015) 565–582. doi:10.3109/10715762.2014.1000318.

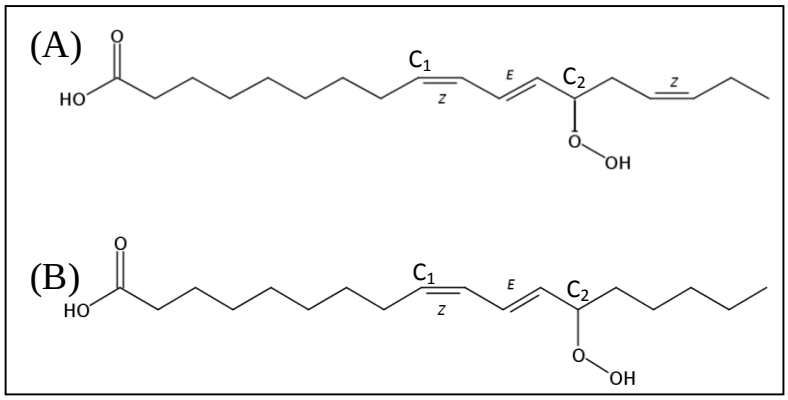

Figure 1: Chemical structure of 13-HPOT (A) and 13-HPOD (B).

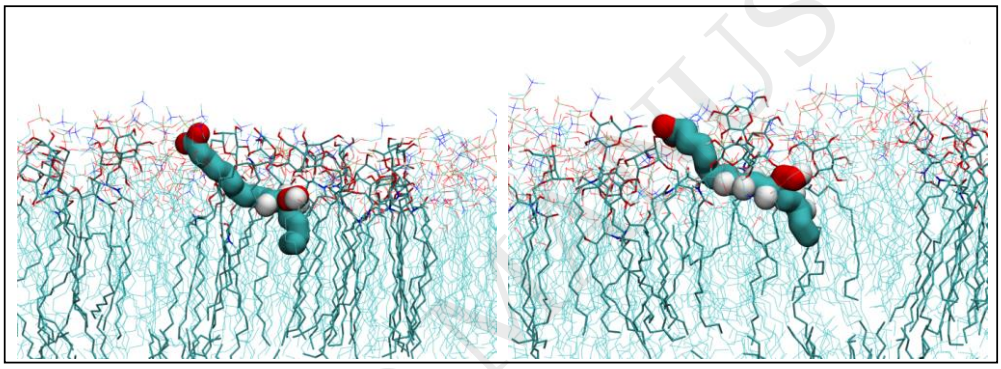

Figure 2: Representative conformation of HPOD (left panel) and HPOT (right panel) in a membrane of PLPC/Sitosterol/GluCer (60/20/20) (288 molecules). For clarity, only half bilayer is represented and double bond hydrogens have been added. The image shows one HPOD or HPOT molecule after 1 µs simulation.

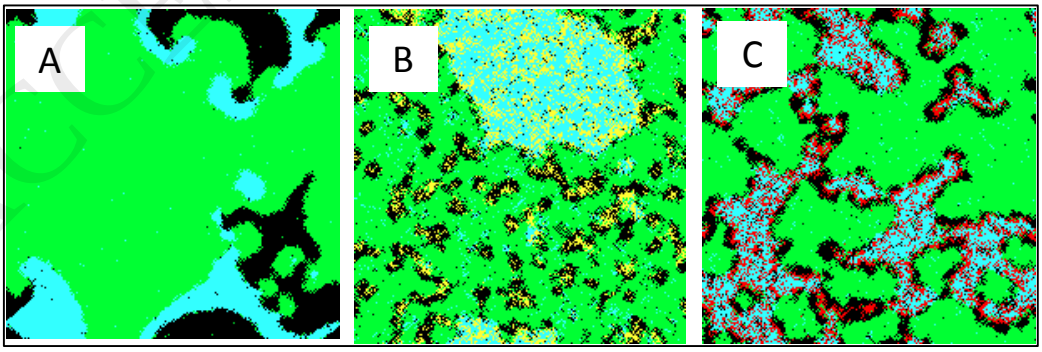

Figure 3: Monolayer grid of 200×200 lipids calculated by the BM procedure. Each pixel represents a molecule, green: PLPC, black: sitosterol, blue:GluCer, yellow: HPOT and red; HPOD. A) PLPC/sitosterol/GluCer monolayer at 60:20:20 molar ratio in the absence of HPOs, B) PLPC/sito/GluCer/HPOT monolayer at 54:17:17:12 molar ratio, C) PLPC/sitosterol/GluCer/HPOD monolayer at 54:17:17:12 molar ratio.

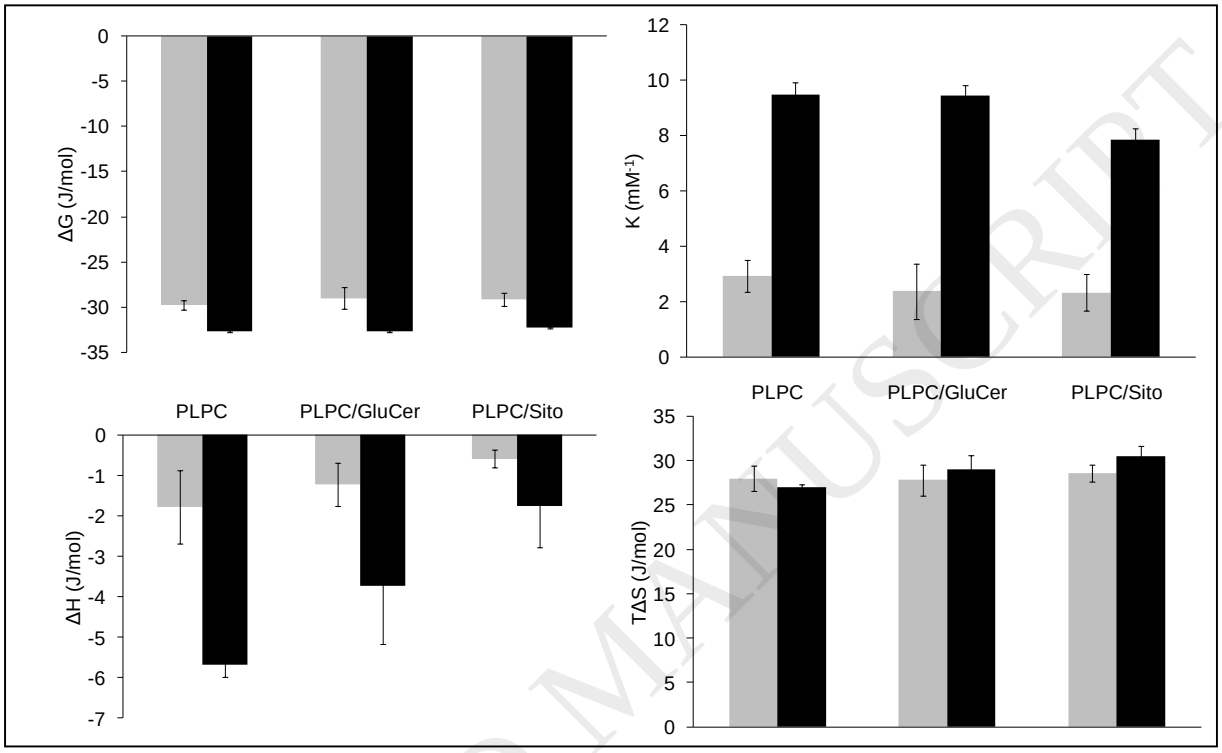

Figure 4: Thermodynamic parameters for the binding of HPOs with simplified liposomes. ΔG = Molar free energy change, K = binding coefficient, ΔH = molar enthalpy change and TΔS molar entropy change of the interactions of HPOs with liposomes composed of PLPC or PLPC/sitosterol or PLPC/GluCer. Black bars: HPOT, Grey bars: HPOD.

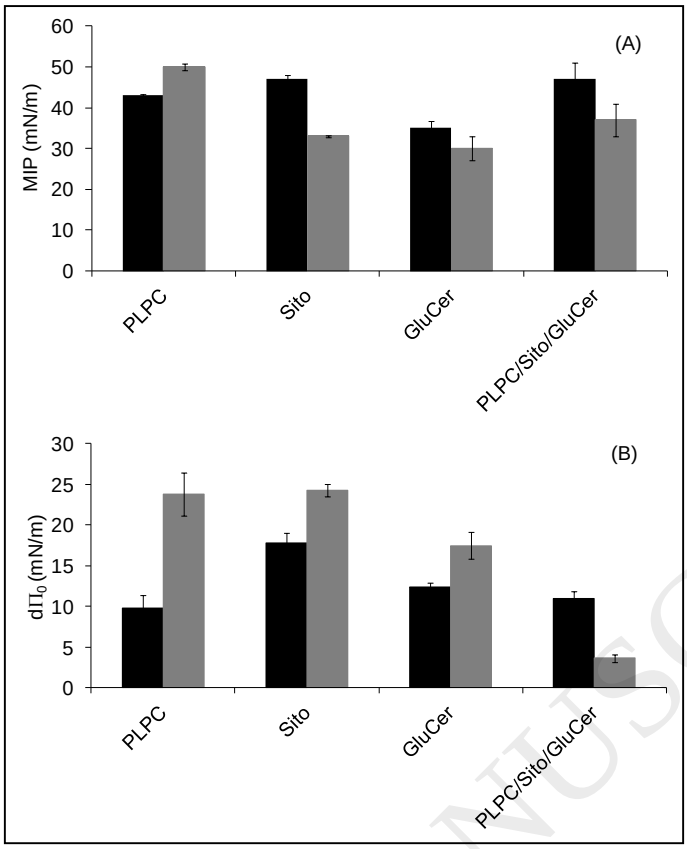

Figure 5: Adsorption of HPOs into lipid monolayers. (A) Maximal insertion pressure (MIP) and (B) differential Π_0 ($d\Pi_0$) values for HPOT in black and HPOD in grey. These parameters are described in the Material and Methods section.

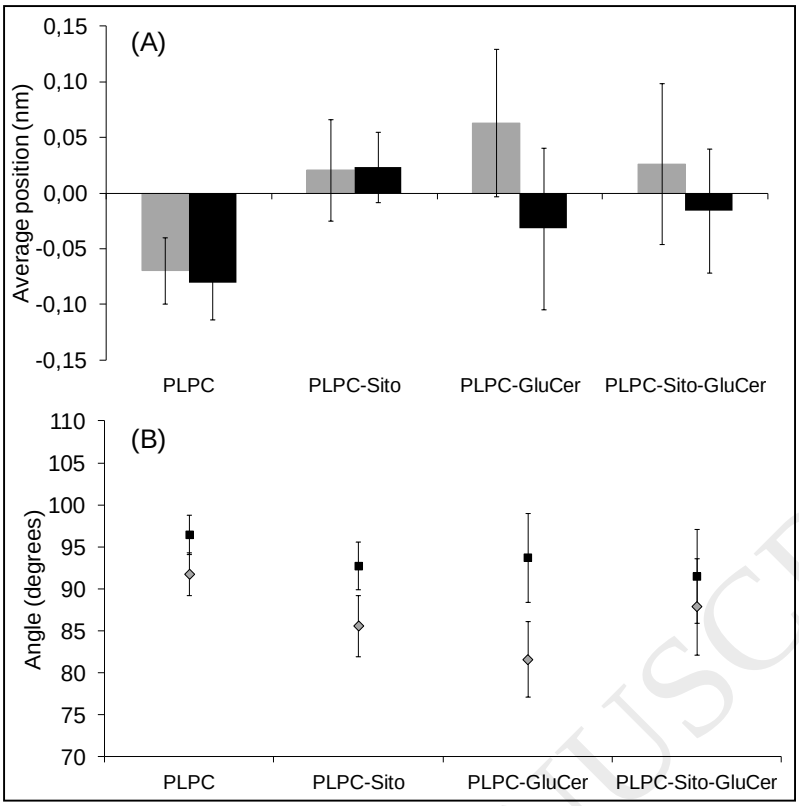

Figure 6: (A) Relative position of the acid group of HPOs against the average PO4 position of PLPC in the different lipid compositions tested. Black bars= HPOT and grey bars= HPOD, (B) Angle between the two double bonds of HPOs relative to the membrane normal. Black diamond= HPOT and grey square= HPOD

Table 1. Comparison of the location of the IR Bands (cm^{-1}) between the different systems tested.

	CH_3 asymmetric stretching	*CH_2 asymmetric stretching*	*CH_2 symmetric stretching*	*P=O asymmetric stretching*	*C=O ester stretching*
PLPC	2956	2923.5	2854	1226	1732
PLPC-HPOT	2955	2921	2852	1218	1733
PLPC-HPOD	2955	2921	2852	1228	1733
PLPC-sito	2954	2921	2852	1226	1737
PLPC-sito HPOT	2954	2921	2852	1226	1737
PLPC-sito-HPOD	2954	2921	2852	1220	1737
PLPC-GluCer	2956	2922	2852	1236	1738
PLPC-GluCer-HPOT	2956	2924	2854	1230	1738
PLPC-GluCer-HPOD	2956	2924	2854	1240	1738

The critical micellar concentrations were determined at the intersection between the linear regression of the ascendant and horizontal regions of the curve.